

1 **Electronic Supplementary Material**

2

3 **Gold nanoparticle-doped three-dimensional reduced**

4 **graphene hydrogel modified electrode for amperometric**

5 **determination of indole-3-acetic acid and salicylic acid**

6 Xiaodong Cao,^a Xueting Zhu,^a Shudong He,^a Xuan Xu,^b Yongkang Ye,^{*a} Sundaram

7 Gunasekaran,^{*c}

8 *^a School of Food and Biological Engineering, Hefei University of Technology, Hefei*

9 *230009, China. E-mail: yongkang.ye@hfut.edu.cn*

10 *^b School of Chemistry and Molecular Engineering, Nanjing Tech University, Nanjing*

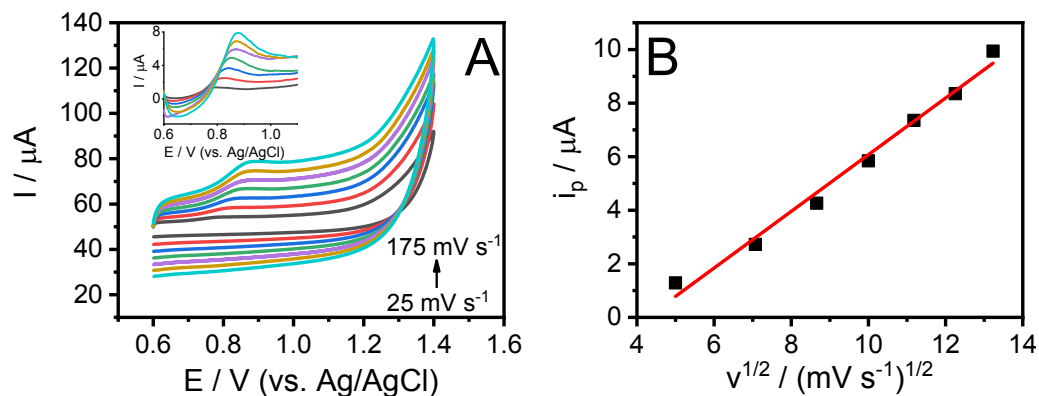
11 *211816, China*

12 *^c Department of Biological Systems Engineering, University of Wisconsin-Madison,*

13 *Madison, WI 53706, USA. E-mail: guna@wisc.edu*

15 The effect of scan rate on the oxidation of IAA on AuNPs-GH/GCE

16



17

18

19 **Fig. S1** Cyclic voltammograms (CVs) of AuNPs-GH/GCE in 0.1 mol L⁻¹ PBS (pH

20 2.5) containing 80 μM IAA at various scan rate (from bottom to top: 25, 50, 75, 100,

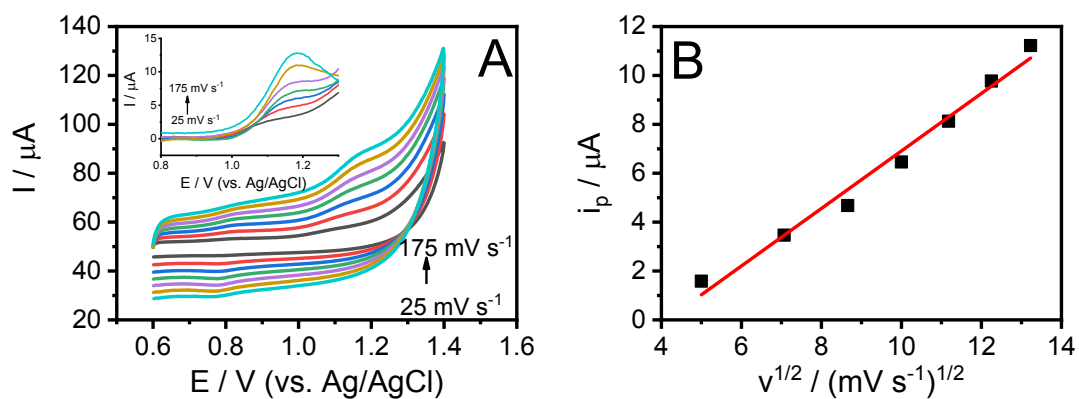
21 125, 150 and 175 mV s⁻¹). Inset: the first segments of the corresponding CVs

22 corrected by background subtraction. (B) Plots of the anodic peak currents vs. square

23 root of scan rate (v^{1/2}).

25 The effect of scan rate on the oxidation of SA on AuNPs-GH/GCE

26



27

28

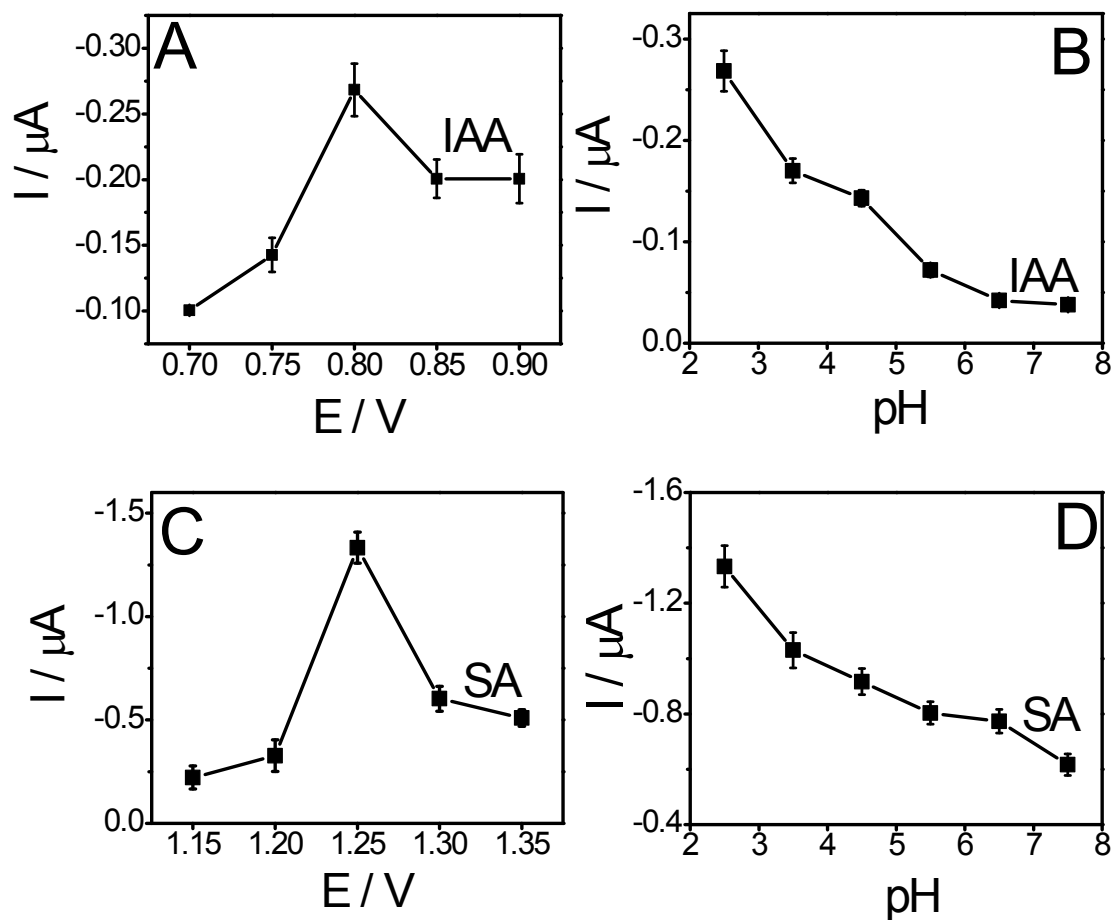
29 **Fig. S2** CVs of AuNPs-GH/GCE in 0.1 mol L⁻¹ PBS (pH 2.5) containing 60 μM SA at

30 various scan rate (from bottom to top: 25, 50, 75, 100, 125, 150 and 175 mV s⁻¹). Inset:

31 the first segments of the corresponding CVs corrected by background subtraction. (B)

32 Plots of the anodic peak currents vs. square root of scan rate ($v^{1/2}$).

33 Parameter optimization for amperometric detection of IAA and SA

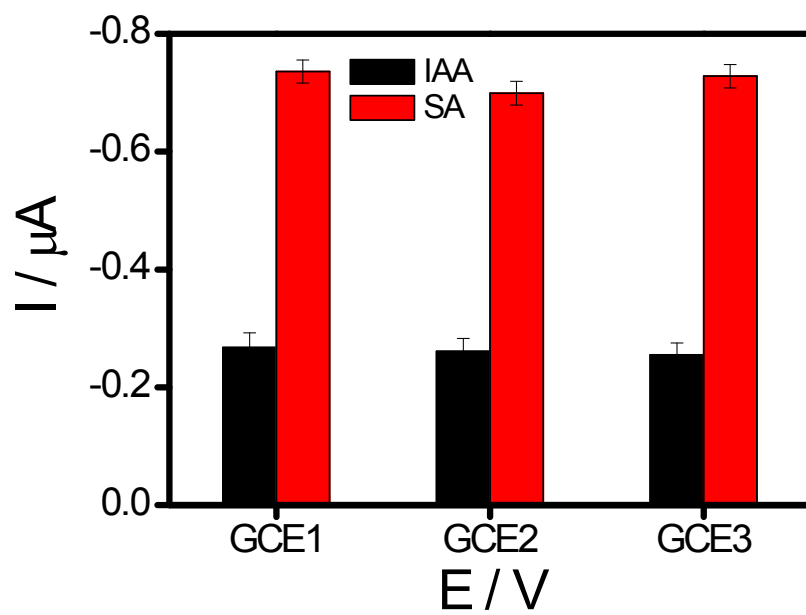


34

35 **Fig. S3** Work potential optimization for amperometric detection of IAA (A) and SA

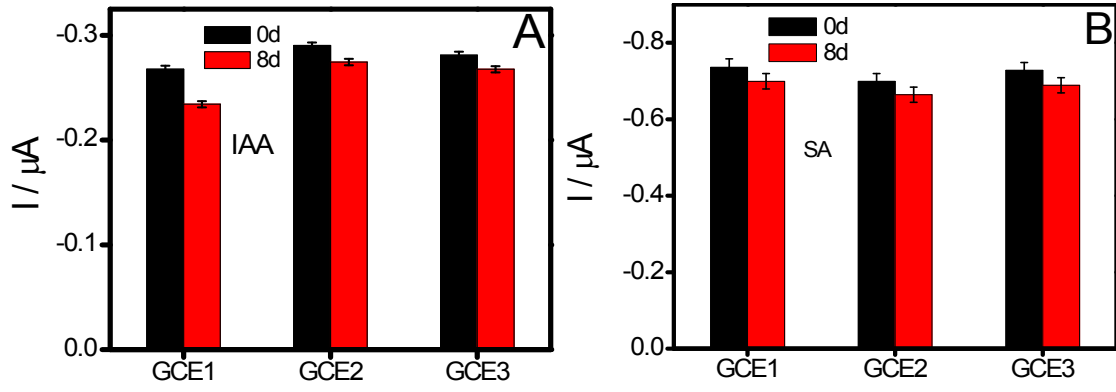
36 (C). The pH value optimization for amperometric detection of IAA (B) and SA (D).

37 The concentrations of IAA and SA were 20 μM .



39

40 **Fig. S4** The fabrication reproducibility of the sensors.



42

43 **Fig. S5** Stability of the sensors.

45 **Table S1** The average particle size of AuNPs in GHs prepared under various
46 temperature. The data were obtained from XRD associated to Au (111) plane.

Reaction temperature / °C	Particle size / nm
100	14.5
120	14.9
140	15.2
160	16.6
180	17.9

48 **Table S2** The calculated d-spacing value of the C (002) plane of AuNPs-GHs
49 prepared at various temperature and GH at 140 °C.

Reaction temperature / °C	2 θ / °	d-spacing / nm
100	21.03	0.422
120	23.92	0.372
140	24.87	0.357
160	24.90	0.357
180	25.40	0.350
GH-140	23.10	3.890

51

Table S3 Results of the recovery analysis of IAA and SA in unknown samples ($n = 3$)^a

Group	IAA added (μM)	SA added (μM)	IAA detected (μM)	SA detected (μM)	IAA recovery (%)	SA recovery (%)
1	a	b	1.35	2.01	95.50 \pm 5.98	96.95 \pm 4.53
	0.5	0.50	1.77 \pm 0.11	2.43 \pm 0.11		
	c	d	3.11	3.28		
2	5	5	7.75 \pm 0.19	7.86 \pm 0.18	95.60 \pm 2.29	94.93 \pm 2.15
	e	f	2.38	2.26		
3	15	15	17.58 \pm 0.39	16.96 \pm 0.73	101.15 \pm 2.22	98.26 \pm 4.21

52 ^a values reported are the averages of three independent analyses of each spiked sample.